3D Model Based on Terrestrial Laser Scanning (TLS) Case study: The Cangkuang Temple, Garut District, West Java, Indonesia

Sadikin Hendriatiningsih[1], Deni Suwardhi[2] & Januragadi[3]

[1] Survey and Cadastre Research Group,
Faculty of Earth Science and Technology, Institute of Technology Bandung,
[2] Remote Sensing and Geographical Information Systems Research Group,
Faculty of Earth Science and Technology, Institute of Technology Bandung
[3]Alumni of Geodetic & Geomatics Engineering Program,
Faculty of Earth Science and Technology, Institute of Technology Bandung
Jalan Ganesa No.10, Bandung 40132, Indonesia
Email: hningsih@gd.itb.ac.id

Abstract. The subject of the investigation reported in this paper is the visualization of three-dimensional (3D) surface models in a 3D mapping survey using terrestrial laser scanning (TLS). The Cangkuang Temple nearby Garut City was chosen as the object. The laser technology instruments used were a Topcon GLS-1000 (Geodetic Laser Scanner) and a Topcon IS (Image Station). Twelve points at the same position in each 3D surface model were selected. The coordinate system of the IS was then transformed into the coordinate system of the GLS-1000 using a 3D similarity transformation model. The 3D distances were calculated for each model. Differences in distance were considered as errors in the x, y, and z direction. The standard deviation of the distance differences was ±0.301 m. Some of the distance differences did not fall within the range of tolerances (about 15%). The 3D surface model visualization of the Cangkuang Temple that was created from the GLS-1000 data was more precise than the one created from the IS data. In the future, such 3D surface model visualizations could be used for documentation, preservation and reconstruction of heritage buildings.

Keywords: *3D surface model; coordinates transformation; distance; laser scanner; TLS; visualization.*

1 Introduction

Laser scanning is one of the latest techniques applied in 3D survey and mapping. Currently it is the leading survey technology providing spatial data information. Laser scanning is a process of recording precise 3D information of real world objects or environments. There are many types of measuring instruments that use laser scanning technology with a range of capabilities for a variety of applications [1]. Laser scanning data have a high quality and can be

Received April 25th, 2014, 1st Revision September 24th, 2014, 2nd Revision October 29th, 2014, Accepted for publication November 26th, 2014.
 ISSN: 2337-5779, DOI: 10.5614/j.eng.technol.sci.2015.47.1.1

used in various fields, including topographic surveys and industrial environments. The raw data of the spatial information consist of data points in a point cloud system, numbering in the thousands, which can be processed and edited to create digital surface model visualizations, e.g. digital terrain models (DTM), 3D city models, road models, electricity channel models, 3D object models for cultural heritage preservation and historical documentation, etc. The main advantage of using laser scanning as survey technique is that it provides complete facility in data acquisition and that it delivers 3D data. Robotic technology allows the operator to control the instrument from a distance by remote control. Robotic instruments can also automatically and repeatedly measure targets and store the values in memory without the need of an operator. In addition, the data are obtained quickly, so costs can be reduced significantly [2]. Modeling technology for the visualization of cultural heritage objects is currently supported by laser-scanning and robotic technologies. Cultural heritage preservation is very important and therefore cultural heritage objects, such as temples and statues, should be noted and documented in detail. This is necessary in order to be able to reconstruct these objects. Laser scanning technology can be used for modeling, 3D visualization and imagery as forms of documentation [3].

In recent years, the number of cultural heritage buildings that were documented using 3D survey technology has increased. For example, Altuntas and Yildiz [3] used automation applications for laser scanning the cultural heritage building of Al-Khasneh in the ancient city of Petra, the capital of the Nabataean Kingdom from 400 BC to AD 106, located in southwestern Jordan. The building is often referred to as the eighth wonder of the world, along with the theater buildings in the nearby Roman city of Jerash. Constructed in the 2nd century BC it is one of the best preserved ancient buildings in the world. Karabork, *et al*. [4] applied alternative modeling, visualization and imaging techniques to a Roman sarcophagus from AD 250-260 using a reflector-less robotic total station survey instrument, with modeling done using commercial software. Grussenmeyer, *et al*. [5] compared data acquisition methods of tacheometry measurement, photogrammetry and terrestrial laser scanning to record the cultural heritage building of Castle Haut-Andlau (Alsace, France), which was built in the middle ages and documented in the years 2006-2008. Cheong, *et al*. [6] present a research case study regarding cultural heritage documentation of the historic building Istana Lama Seri Menanti in the royal capital of Negeri Sembilan, Malaysia. Rasztovits and Dorninger [7] concluded that for very accurate 3D modeling documentation, the TLS method should be used to reconstruct surface geometric objects.

The culture of a nation cannot be separated from its historical heritage as a symbol of its identity. Maintenance and preservation of cultural heritage objects

such as archeological sites, temples, museums and cultural parks is necessary because they are an important part of the cultural wealth of a nation. International attention for the existence of sites of high cultural and historical value in Indonesia is evident. The United Nations Educational Scientific and Cultural Organization (UNESCO) [8] tries to identify, protect and preserve cultural and natural heritage objects around the world that provide outstanding value to humanity. This is stated in the international treaty called the *Convention concerning the Protection of World Cultural and Natural Heritage*, adopted by UNESCO in 1972. It encourages countries to sign the World Heritage Convention and to nominate sites within their national territory for inclusion on the World Heritage List. Therefore, the attention of UNESCO should be appreciated, especially in Indonesia.

The history of temples in Indonesia [9] is inseparable from the history of kingdoms, because the construction of a temple in the past happened in order of a king or a head of government of the nation that occupied the area where the temple was located. After the Dutch colonial era very few ancient relics have been found in West Java. Several historical sites, such as the ruins of ancient buildings in several places in West Java, were discovered about thirty years ago. The Cangkuang Temple is the only temple that has been restored in West Java. It is located in Cangkuang Village, Leles subdistrict, Garut District, West Java, Indonesia (Figure 1).

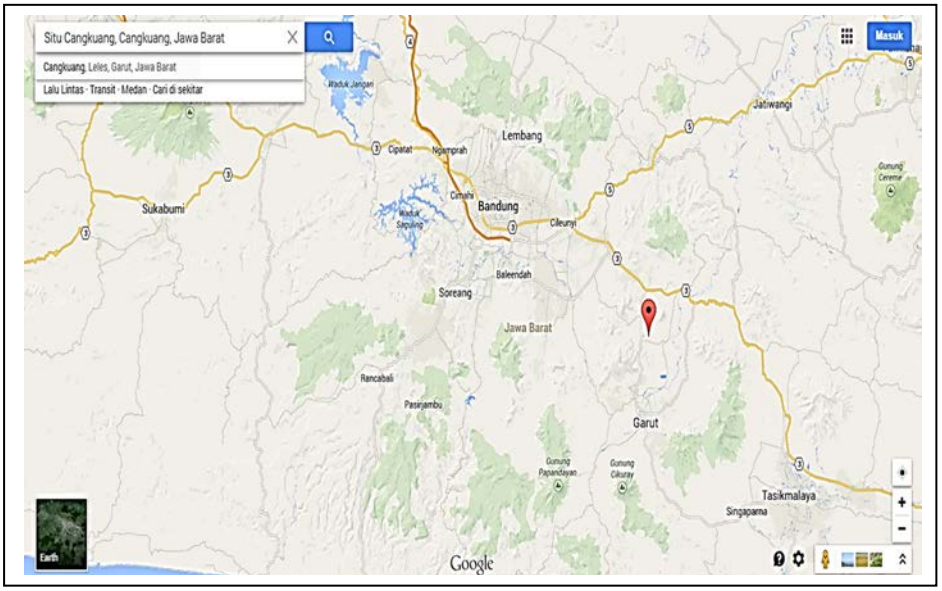

Figure 1 Garut District, West Java, Indonesia [10].

The temple is located on a small island that extends from west to east with an area of approximately 16.5 hectares. The island is located in the middle of a small lake (called *situ* in Sundanese) surrounded by mountains. To reach the site visitors must cross the water using a raft (Figure 2). The lake's position is at 106° 54' 36.79" east longitude, 7° 06' 09" south latitude and at an altitude of about 600 m above mean sea level.

Figure 2 Situ Cangkuang [10].

Right beside Cangkuang Temple there is a settlement called Kampung Pulo that was originally surrounded by the lake. At present only the northern part is at the lake, since the southern part was turned into rice fields. Kampung Pulo is a traditional Sundanese settlement and it was included in the cultural heritage area together with the temple because its history and location are unique. Many domestic and foreign tourists visit the site. The Garut District Government has designated the area for cultural and natural tourism.

Figure 3 Cangkuang Temple [10].

This paper discusses available laser scanner technologies and a comparison by point position of 3D surface models of Cangkuang Temple (Figure 3) that were obtained using two laser technology instruments: a Topcon GLS-1000 (Geodetic Laser Scanner), which is a robotic long-range scanning instrument, and a Topcon Image Station (IS), which is a robotic imaging total station. Analysis was performed of the results of the 3D surface visualization model and specifically of the differences in spatial distance between the 3D surface models generated by each instrument.

2 Terrestrial Laser Scanning

A terrestrial laser scanner (TLS) is an automatic, ground-based device that uses a laser to measure the 3D coordinates of a given region of an object's surface in a systematic order and at a high rate in near real time [11]. 3D TLS is a relatively new surveying technique. In TLS, instruments are categorized by principle of distance measurement [12]. The distance measurement principle correlates to both the range and the resulting accuracy of the system. The three principal types of scanning technology systems are based on time of flight (TOF), phase shift, and triangulation respectively. Of these three the technique that is most commonly used for outdoors geodetic surveying or measuring building structures is the TOF technique [13].

In a TOF system, a laser pulse is sent out and a portion of the pulse is reflected from a given surface and returns to the unit (Figure 4). The distance to the surface is calculated from the time of flight of the pulse. The distance to the surface can be calculated using the following formula [14]:

$$D = \frac{(c.t)}{2} \tag{1}$$

with c = speed of light in air (m/sec)
t = time between sending and receiving the signal (sec)

The raw observables in TLS are: range (r), horizontal direction (φ) and vertical angle (θ) (Figure 5). Many scanners also record the intensity of the reflected laser signal at each point, which is thus the fourth observable. By scanning the scene, one obtains a large collection of densely spaced and regularly sampled points (point cloud), which may contain as many as several thousands of points. The point cloud is a collection of XYZ coordinates in a common reference system that portrays to the viewer an understanding of the spatial distribution of a subject or site [11].

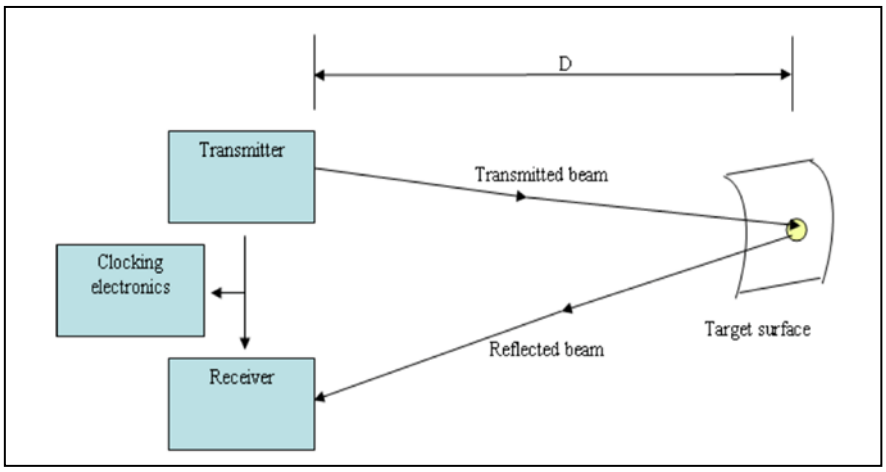

Figure 4 Time-of-flight laser scanner principle [14].

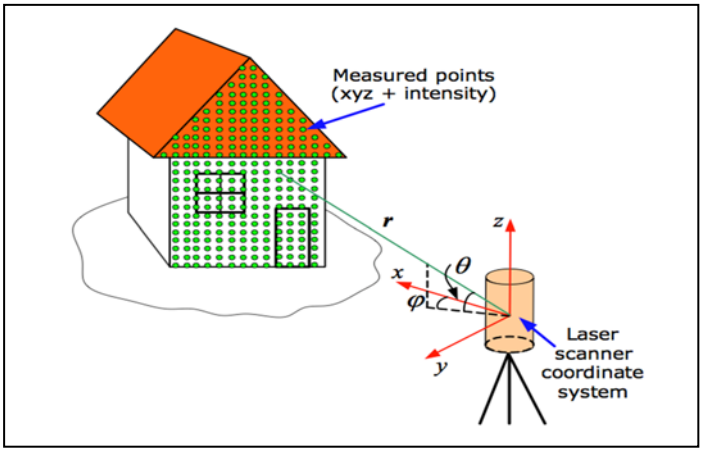

Figure 5 The principle of TLS and laser scanner observables [11].

The relationship between the raw observables (r, φ, θ) and the coordinates (x, y, z) can be expressed as follows [11]:

$$\mathbf{X_i} = \begin{bmatrix} x_j \\ y_j \\ z_j \end{bmatrix} = \begin{bmatrix} r_j cos\varphi_j cos\theta_j \\ r_j sin\varphi_j cos\theta_j \\ r_j sin\theta_j \end{bmatrix} \quad (2)$$

where r_j, φ_j and θj are the measured range, horizontal direction and vertical angle, respectively, to the ***j***-th point in the point cloud, while (x_j, y_j, z_j) are its rectangular (Cartesian) coordinates in the scanner (instrument-fixed, designated by the subscript ***i*** in $\mathbf{X_i}$) coordinate system. Point clouds obtained from each

setup are referenced to the instrument-fixed i.e. internal coordinate system of the scanner (Figure 6). This coordinate system can be defined as follows:

- origin: at the instrument's electro-optical center,
- *z*-axis: along the instrument's vertical (rotation) axis,
- *x*-axis: along the instrument's optical axis with an arbitrary horizontal angle,
- *y*-axis: orthogonal to the two previous axes, so that a right-hand system is formed.

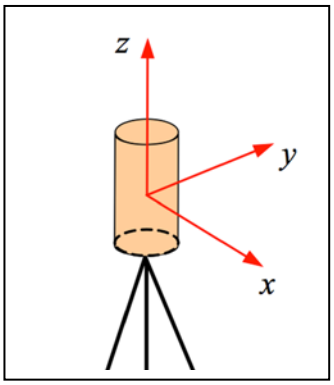

Figure 6 Laser scanner coordinate system [11].

In general, multiple scanning positions are necessary to cover the entire surface of an object. To obtain a complete representation of the scanned object, the different point clouds should be transformed into a common coordinate system, i.e. the coordinate system of a chosen scan. This procedure is called *registration*, whereby the registered scans are combined in one dataset [11].

Hence, transformation between the different scans is required. The transformation (Eq. 3) consists of 7 parameters – 3 rotation angles (R), 3 translations (T) and a scale (m) [15]:

$$\boldsymbol{X} = \boldsymbol{m} * \boldsymbol{R} * \boldsymbol{x} + \boldsymbol{T} \tag{3}$$

In [1] it is explained that registration is the transformation of multiple scans into a common coordinate system (CS), the CS of a chosen scan. Take two scans of an object taken from different positions. In order to be able to register the two scans they should have an overlap. In order to transform the CS of Scan 2 into the CS of Scan 1, one must determine the transformation parameters of the two coordinate systems, as depicted in Figure 7.

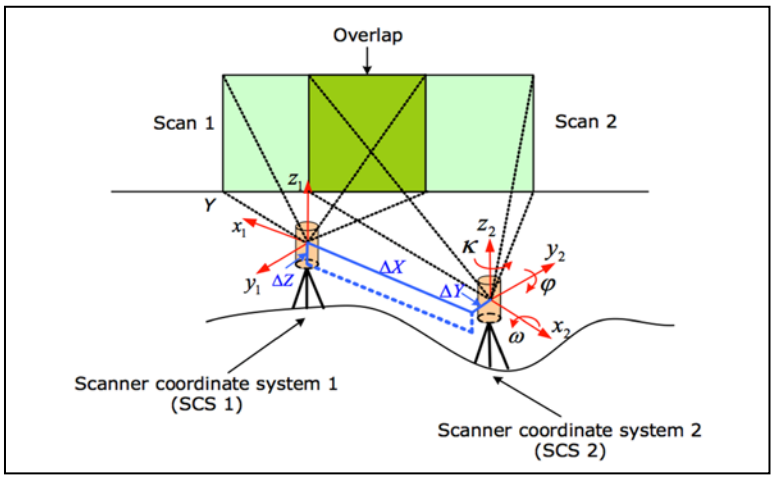

Figure 7 Registration of two scans [11].

The transformation parameters are 3 translations along 3 coordinate axes (ΔX, ΔY, ΔZ) and 3 rotations around the 3 coordinate axes (ω, ϕ, κ) called the rigid-body transformation parameters (i.e. no scale factor). This transformation is also called a 3D Helmert transformation without a scale factor. In order to be able to integrate the TLS data into geospatial data, the registered point cloud of the whole object has to be transformed into a geodetic coordinate system (local or national). This procedure is called *geo-referencing* [11].

In this study, performing *direct registration* means that the position and orientation of the scanner were directly computed using the software of the respective instruments.

Point cloud processing means a process of transforming the raw registered point cloud into a final deliverable. These deliverables come in a wide variety of formats: cleaned point cloud data, standard 2D drawings and fully 3D texture models. Through 3D point cloud processing, the deliverables can be extracted straight away by creating a 3D surface model from the point cloud. In data improvement, the first step in the meshing process is removing noisy data from the point cloud [14]. The product from the 3D modeling process is a meshed surface model that is created by connecting all the obtained points in the point cloud with small triangles. In this way a surface model or mesh is generated. This mesh is the interpolation of the points in three dimensions, which creates a full surface representation.

The Topcon GLS-1000 [15] is a pulse-based laser scanner designed to manage the practical aspects of the job site. With a scan range of up to 330 m, the GLS-

1000 is a versatile tool that allows laser scanning in many different work environments. It is a robust scanner that sends out a laser beam that measures 3000 points per second (pts/sec). The GLS-1000 has the ability to input, occupy and back-sight known real-world coordinates on board. Its operation requires no need to bring a Total Station to locate positions for point cloud registration later at the office, because it has the ability to input known points, elevations and back-sight, so the point clouds obtained can be registered in the field. The GLS-1000 is equipped with ScanMaster software, which is used for scanning control, 3D visualization and point cloud registration. The scanned data can be exported in a wide variety of file formats for compatibility. However, in this study the Cyclone 5.5 software was used. For the 3D surface model visualization AutoCAD LDD 2009 was used.

Topcon GLS-1000 Topcon Imaging Station

Figure 8 Topcon GLS-1000 [15] and Topcon Imaging Station [16].

The Topcon Imaging Station (IS) [16] is a scanning, robotic, reflector-less imaging station. Topcon's IS combines the best of two worlds: advanced imaging and high-accuracy surveying, incorporating real-time field imagery with spatial data. The IS's functionality is controlled using Topcon Image Master software. The high-speed measurement grid scan obtains 3D data by automatically scanning at a specified pitch within a specified area. Using Topcon's image analyzing software, 3D models can be created from the data. Intelligent Scan automatically recognizes significant features in the images. Its 20 pts/sec scan rate and its 2000 m precision reflector-less range are ideal for most applications. With Topcon Image Master software, triangulated irregular network (TIN) images can be formed from 3D point cloud data and it is

possible to create texture-mapped 3D models of objects. Additionally there are Image Drive, for visually operating the instrument from the controller and easily switching from imaging to prism tracking, and Independent Control, for allowing complete control from a computer, WiFi and compatible devices.

Both laser instruments are shown in Figure 8.

Each instrument's capabilities are summarized based on the technical specifications issued by the manufacturer (Figure 9).

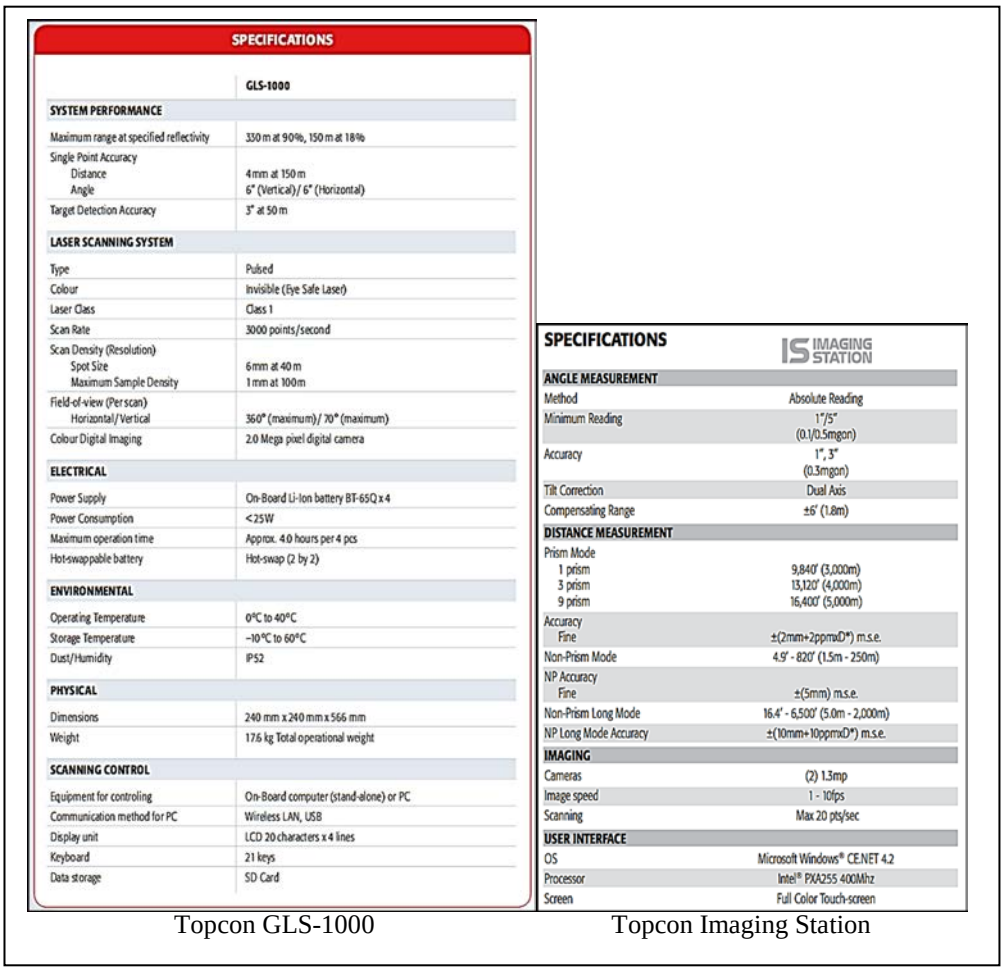

SPECIFICATIONS

	GLS-1000
SYSTEM PERFORMANCE	
Maximum range at specified reflectivity	330 m at 90%, 150 m at 18%
Single Point Accuracy Distance Angle	 4 mm at 150 m 6" (Vertical) / 6" (Horizontal)
Target Detection Accuracy	3" at 50 m
LASER SCANNING SYSTEM	
Type	Pulsed
Colour	Invisible (Eye Safe Laser)
Laser Class	Class 1
Scan Rate	3000 points/second
Scan Density (Resolution) Spot Size Maximum Sample Density	 6 mm at 40 m 1 mm at 100 m
Field-of-view (Per scan) Horizontal / Vertical	 360° (maximum) / 70° (maximum)
Colour Digital Imaging	2.0 Mega pixel digital camera
ELECTRICAL	
Power Supply	On-Board Li-Ion battery BT-65Q x 4
Power Consumption	<25W
Maximum operation time	Approx. 4.0 hours per 4 pcs
Hot-swappable battery	Hot-swap (2 by 2)
ENVIRONMENTAL	
Operating Temperature	0°C to 40°C
Storage Temperature	-10°C to 60°C
Dust/Humidity	IP52
PHYSICAL	
Dimensions	240 mm x 240 mm x 566 mm
Weight	17.6 kg Total operational weight
SCANNING CONTROL	
Equipment for controling	On-Board computer (stand-alone) or PC
Communication method for PC	Wireless LAN, USB
Display unit	LCD 20 characters x 4 lines
Keyboard	21 keys
Data storage	SD Card

SPECIFICATIONS IS IMAGING STATION

ANGLE MEASUREMENT	
Method	Absolute Reading
Minimum Reading	1"/5" (0.1/0.5mgon)
Accuracy	1", 3" (0.3mgon)
Tilt Correction	Dual Axis
Compensating Range	±6' (1.8m)
DISTANCE MEASUREMENT	
Prism Mode 1 prism 3 prism 9 prism	 9,840' (3,000m) 13,120' (4,000m) 16,400' (5,000m)
Accuracy Fine	 ±(2mm+2ppmxD*) m.s.e.
Non-Prism Mode	4.9' - 820' (1.5m - 250m)
NP Accuracy Fine	 ±(5mm) m.s.e.
Non-Prism Long Mode	16.4' - 6,500' (5.0m - 2,000m)
NP Long Mode Accuracy	±(10mm+10ppmxD*) m.s.e.
IMAGING	
Cameras	(2) 1.3mp
Image speed	1 - 10fps
Scanning	Max 20 pts/sec
USER INTERFACE	
OS	Microsoft Windows® CE.NET 4.2
Processor	Intel® PXA255 400Mhz
Screen	Full Color Touch-screen

Topcon GLS-1000 Topcon Imaging Station

Figure 9 Topcon GLS-1000 [15] and Topcon Imaging Station [16] specifications.

3 Methods and Results

First, scan-stations were set up around the temple at 5 fixed points (Figure 10). Scanning from the scan-stations was done with both instruments, the GLS-1000 and IS. The GLS-1000 was able to scan the entire object from 4 scan-stations, while the IS required 5 scan-stations to obtain the overlapping point clouds needed to create a 3D model.

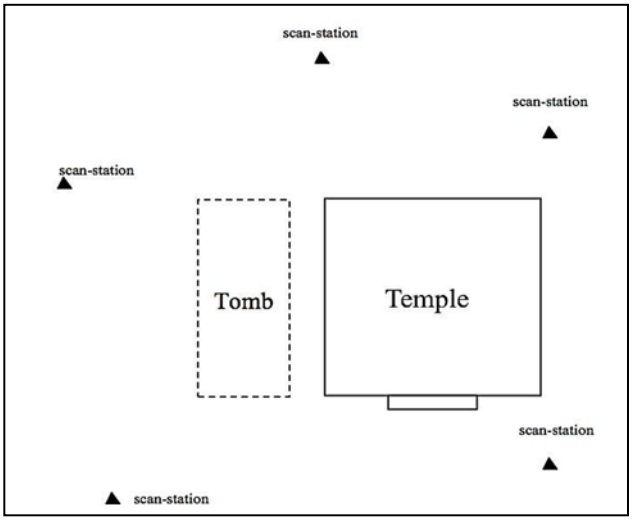

Figure 10 Scan-stations around the temple.

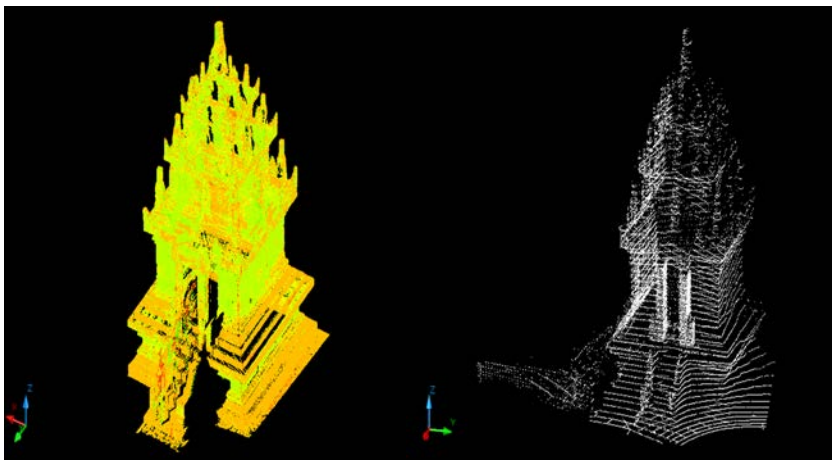

GLS-1000 data IS data

Figure 11 3D space model visualization.

Scanning with the GLS-1000 was done using Cyclone 5.5 software with the grid scan method, while with the IS it was done using TopSurv software. The scan rate was 20 pts/sec for the IS and 3000 pts/sec for the GLS-1000. The point cloud density setting was 10 mm for the IS and 2 mm for the GLS-1000, resulting in 3D solid model visualizations as shown in Figure 12. During processing, the point clouds from the different scan positions were linked together and were registered subsequently.

After scanning, all point cloud data were downloaded. The data from each instrument were stored in AutoCAD format.

The AutoCAD 2009 software was used to obtain a visualization of the 3D model from each instrument. One of the first results was a realistic illustration of the temple (Figure 11).

Filtering was done manually, i.e. by identifiying objects that are not needed and removing them, such as a tree or other objects. The geo-referencing process was not performed, because the point cloud data from both instruments have their own coordinate systems.

A 3D solid model was obtained using the Rapidform 2006 software and the created visualization of the 3D solid model was compared with a photographic image of the temple. For comparison, the 3D solid model visualizations from each instrument are shown along with a photographic image in Figure 12.

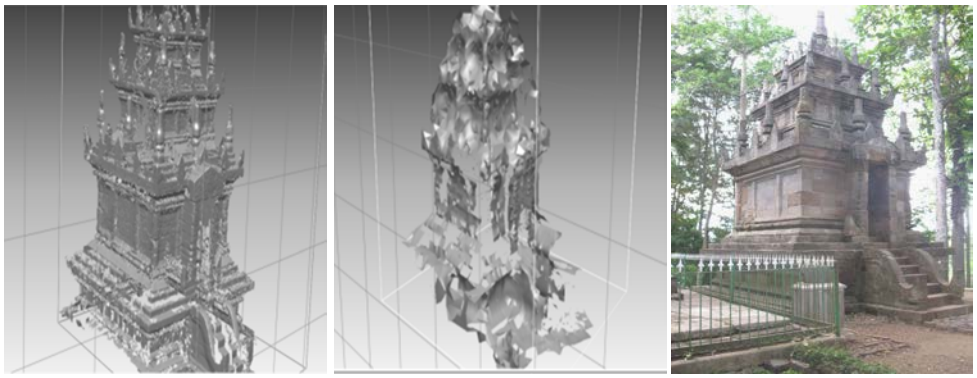

Figure 12 3D surface model and photographic image of temple.

Next, twelve points were selected with the same point position in both 3D models. A sample of the selected points on the object is shown in Figure 13.

Figure 13 Selected points on temple.

The 3D coordinate values of the twelve selected points from each 3D model derived from the GLS-1000 and IS data sets were determined using the AutoCAD 2009 software. The results are shown in Table 1.

Table 1 Points Coordinates of the Object on the 3D Model.

Point number	GLS 1000 Coordinate			IS Coordinate		
	x (m)	y(m)	z(m)	X(m)	Y(m)	Z(m)
1	17.896	26.966	-2.979	30.375	37.083	0.174
2	17,968	26.968	-1.828	30.308	37.031	1.311
3	19.552	28.395	-3.001	31.754	35.380	0.216
4	21.042	28.377	-2.997	31.662	33.922	0.218
5	20.989	26.893	-2.962	30.178	33.993	0.209
6	22.504	26.839	-2.964	30.071	32.401	0.237
7	22.553	26.780	-1.842	30.013	32.448	1.301
8	21.022	26.630	-1.054	29.851	34.025	2.141
9	20.549	26.698	0.161	29.918	34.474	1.562
10	20.556	26.659	-1.774	29.924	34.493	3.399
11	19.944	26.655	0.138	29.950	35.078	3.366
12	19.447	26.647	-1.042	29.967	35.585	2.122

The IS coordinate system was transformed into the GLS-1000 coordinate system. A 3D similarity model transformation was used (Eq. 3), which consists of 7 parameters: 3 rotation angles (R), 3 translations (T) and a scale (m). Three is the minimum number of common points required in order to solve for the seven transformation parameters. In this study, four common points were used and a least-square solution was applied.

$$\begin{bmatrix} X \\ Y \\ Z \end{bmatrix} = m\,R \begin{bmatrix} x \\ y \\ z \end{bmatrix} + \begin{bmatrix} T_x \\ T_y \\ T_z \end{bmatrix} \tag{4}$$

where:

X, Y, Z = point coordinate after transformation
x, y, z = point coordinate to be transformed
m = scale factor
R = 3×3 orthogonal rotation matrix
($\boldsymbol{T_x}$, $\boldsymbol{T_y}$, $\boldsymbol{T_z}$) = coordinates translation of the origin of the ***xyz*** coordinates in the ***XYZ*** frame.

The rotation matrices about the ***x, y,*** and ***z*** axes are:

$$Rz(\boldsymbol{\kappa}) = \begin{bmatrix} \cos\kappa & \sin\kappa & 0 \\ -\sin\kappa & \cos\kappa & 0 \\ 0 & 0 & 1 \end{bmatrix} \quad (5)$$

$$Ry(\boldsymbol{\phi}) = \begin{bmatrix} \cos\phi & 0 & -\sin\phi \\ 0 & 1 & 0 \\ \sin\phi & 0 & \cos\phi \end{bmatrix} \quad (6)$$

$$Rx(\boldsymbol{\omega}) = \begin{bmatrix} 1 & 0 & 0 \\ 0 & \cos\omega & \sin\omega \\ 0 & -\sin\omega & \cos\omega \end{bmatrix} \quad (7)$$

$$\boldsymbol{R} = Rz(\boldsymbol{\kappa}).Ry(\boldsymbol{\phi}).Rx(\boldsymbol{\omega}) \quad (8)$$

$\boldsymbol{R}$=

$$\begin{bmatrix} \cos\kappa\cos\phi & \cos\kappa\sin\phi\sin\omega + \sin\kappa\cos\omega & \sin\kappa\sin\omega - \cos\kappa\sin\phi\cos\omega \\ -\sin\kappa\cos\phi & \cos\kappa\cos\omega - \sin\kappa\sin\phi\sin\omega & \sin\kappa\sin\phi\cos\omega + \cos\kappa\sin\omega \\ \sin\phi & -\cos\phi\sin\omega & \cos\phi\cos\omega \end{bmatrix} \quad (9)$$

where $\boldsymbol{\omega}$, $\boldsymbol{\phi}$ and $\boldsymbol{\kappa}$ are the rotation angles in radians about the ***x, y*** and ***z*** axes respectively.

Based on the distribution of the twelve selected points, four representative points, namely points 2, 3, 4, and 7, were selected to be used for calculating the transformation parameters. The results are shown in Table 2.

Table 2 Transformation Parameters.

Transformation parameter	
$\boldsymbol{T_x}$	+4.822456 m
$\boldsymbol{T_y}$	+53.534302 m
$\boldsymbol{T_z}$	-10.210466 m
m	1.012571
$\boldsymbol{\omega}$	-0.23640978 radian
$\boldsymbol{\phi}$	-0.31420253 radian
$\boldsymbol{\kappa}$	-1.59963698 radian

The twelve points from the IS coordinate system were transformed into the GLS-1000 coordinate system using the transformation parameters in Table 2 and thus positions were obtained for the twelve points from the IS coordinate system in the GLS-1000 coordinate system, as displayed in Table 3.

Table 3 Transformation Coordinates.

Point number	IS Transformation Coordinate		
	***X*(m)**	***Y*(m)**	***Z*(m)**
1	18.197	27.375	-0.911
2	17.884	27.088	-1.985
3	19.534	28.352	-2.761
4	20.975	28.198	-3.059
5	20.944	26.770	-2.588
6	22.523	26.605	-2.887
7	22.722	26.882	-1.862
8	21.363	27.057	-0.669
9	20.822	26.960	-1.139
10	21.187	27.540	+0.591
11	20.602	27.581	+0.684
12	19.817	27.233	-0.371

The spatial distances between the twelve points from the GLS-1000 coordinate system and the twelve points from the IS coordinate system were calculated after the transformation had been executed. From the coordinates of the twelve points in the two 3D models within the coordinate system of the GLS-1000, 66 spatial distance values were obtained for each model, as displayed in Table 4.

Table 4 Spatial Distances.

GLS-1000 coordinate	IS coordinate transformation	No	GLS-1000 coordinate	IS coordinate transformation
Spatial distance (m)			Spatial distance (m)	
1.153	1.155	34	2.613	2.677
2.187	2.483	35	2.136	2.290
3.448	3.607	36	3.628	3.715
3.094	3.275	37	3.742	3.812
4.610	4.818	38	3.059	3.082
4.797	4.650	39	1.516	1.616
3.686	3.191	40	1.927	1.924
2.926	2.667	41	1.926	1.985
4.126	3.350	42	1.282	1.466
3.742	2.893	43	3.161	3.280
2.501	1.714	44	3.280	3.388
2.433	2.219	45	2.475	2.530
3.578	3.455	46	1.125	1.080
3.228	3.135	47	2.427	2.544
4.678	4.750	48	2.294	2.465
4.589	4.844	49	3.687	3.841
3.169	3.720	50	4.027	4.171

GLS-1000 coordinate	IS coordinate transformation	No	GLS-1000 coordinate	IS coordinate transformation
Spatial distance (m)			Spatial distance (m)	
2.595	3.060	51	3.617	3.748
3.279	4.213	52	1.728	1.817
2.805	3.841	53	2.007	2.034
1.705	2.522	54	2.831	2.968
1.491	1.480	55	3.278	3.386
2.080	2.126	56	3.211	3.284
3.338	3.464	57	0.864	0.723
3.600	3.624	58	1.301	1.361
3.011	3.066	59	1.608	1.638
2.320	2.495	60	1.576	1.584
3.744	3.825	61	1.935	1.861
3.610	3.688	62	2.006	1.938
2.627	2.654	63	1.323	1.294
1.486	1.504	64	0.613	0.594
2.122	2.228	65	1.637	1.702
2.483	2.493	66	1.281	1.360

4 Analysis and Discussion

According to the spatial distance values between the twelve points from each 3D model (Table 4), the distance differences were calculated. The results are shown in Figure 14.

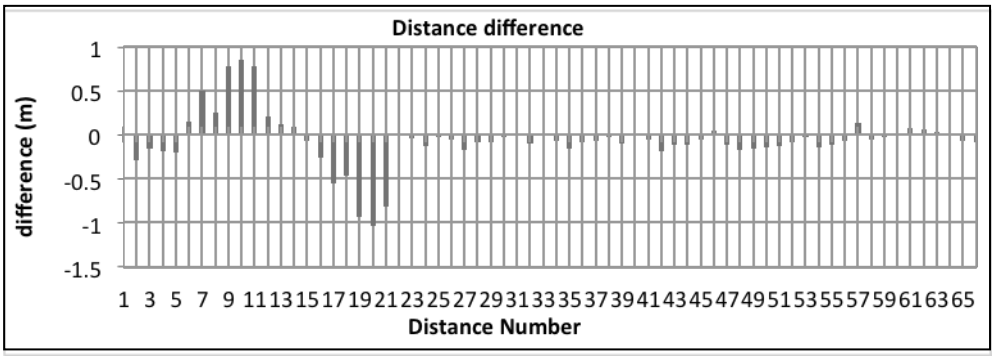

Figure 14 Distance differences.

Distance number 1 had the smallest value (-0.002 m), which was the distance from point 1 to point 2. Distance number 20 had the largest value (-1.036 m), which was the distance from point 2 to point 11. The mean value of the distance differences was -0.061 m and the standard deviation was $\boldsymbol{\sigma_{\Delta d}} = \pm 0.301$ m. Of all of the 66 spatial distances, ten spatial distance numbers were not within the tolerance range, namely the spatial distance numbers 7, 8, 9, 10, 11, 17, 18, 19, 42, 20, and 21.

As a result of the capabilities of each instrument, the object relief of the 3D surface model visualization created from the GLS-1000 data had more detail than that of the model created from the IS data. This is because the density of the point clouds from the GLS-1000 data was denser than that from the IS data. In addition, there are some possibilities that some of the data were deleted in the filtering process.

5 Conclusion

The surveying of culture heritage objects based on laser scanning technology not only reduces the time for fieldwork but also provides 3D surface model visualizations. The object relief of the 3D surface model visualization created with the Topcon GLS-1000 was more detailed than that of the visualization from the Topcon IS. The random error of a number of distance differences did not fit within the range of tolerances – about 15% of all spatial distance differences – because of the possibility that some points from the GLS-1000 model and the IS model were not exactly in the same position while determining the twelve selected points for each model. The results of this study demonstrate that TLS technology can be used for cultural heritage documentation, preservation, and reconstruction of cultural heritage buildings in the future, but for optimal results the TLS technology requires accurate applications and proper instruments. On the basis of this case we recommend the Topcon GLS-1000.

Acknowledgements

Thanks to Mr. Popo from PT. Exsol Innovindo who lent the Topcon GLS-1000 and the Topcon Image Station (IS).

References

[1] Staiger, R., *Terrestrial Laser Scanning-Technology, System and Application*, Proceedings of 2nd FIG Regional Conference, ISBN 87-90907-28-0, Marrakech, Morocco, December 2-5, 2003, Editors: Taïb Tachalait & J. Schnurr, TS 12.3-Positioning and Measurement Technologies and Practices, 2003.

[2] Alkan, R.M. & Karsidag, G., *Analysis of The Accuracy of Terrestrial Laser Scanning Measurements*, Proceedings of FIG Working Week, ISBN 97887-90907-98-3, Commission: 6 and 5-Knowing to Manage The Territory, Protect The Environment, Evaluate The Cultural Heritage, Rome, Italy, 6-10 May 2012, Editors: Prof. Rudolf Staiger & Prof. Volker Schwieger, TS07A – Laser Scanners I, 6097, 2012.

[3] Altuntas, C. & Yildiz, F., *Registration of Terrestrial Laser Scanner Point Clouds by One Image*, XXIst ISPRS Congress Technical Commission VII

July 3-11, 2008 Beijing, China, The International Archives of the Photogrammetry, Remote Sensing and Spatial Information Sciences, Chen Jun, Jiang Jie, Hans-Gerd Maas, (eds.), **XXXVII**(B5), pp. 597-600, 2008.

[4] Karabork, H., Yildiz, F., Yakar, M., Altuntas, C. & Karasaka, L., *Modeling and Visualization using Laser Scanner in Documentation of Cultural Heritage*, Proceeding 21st CIPA Symposium AntiCIPAting the Future of Cultural Past, October 1-6, 2007, Athens, Greece, ISPRS Archives, **XXXVI-5/C53**, 2007.

[5] Grussenmeyer, P., Landes, T., Voegtle, T. & Ringle, K., *Comparison Methods of Terrestrial Laser Scanning, Photogrammetry and Tacheometry Data for Recording of Cultural of Cultural Heritage Buildings*, Proceeding XXIst ISPRS Congress Technical Commission V July 3-11, 2008 Beijing, China, The International Archives of the Photogrammetry, Remote Sensing and Spatial Information Sciences, Chen Jun, Jiang Jie, Hans-Gerd Maas, (eds.), WG V/2 Cultural Heritage Documentation, **XXXVII**(B5), pp. 213-218, 2008.

[6] Cheong, S.C., Ong, C.W., Setan, H., & Majid, Z., *Terrestrial Laser Scanning for Cultural Heritage Documentation, Case Study: The Old Palace, Seri Menanti*, 11th South East Asian Survey Congress and 13th International Surveyors' Congress Innovation towards Sustainability, 22-24 June 2011, Kuala Lumpur, Malaysia, International Office of Cadastre and Land Records (OICRF), http://www.oicrf.org/document.asp?ID=10514. (5 November 2013).

[7] Rasztovits, S. & Dorninger, P., *Comparison of 3D Reconstruction Services and Terrestrial Scanning for Cultural Heritage Documentation*, Proceeding International Archives of the Photogrammetry, Remote Sensing and Spatial Information Sciences, 2013 XXIV International CIPA Symposium, 2-6 September 2013, Strasbourg, France, **XL-5/W2**, 2013.

[8] UNESCO, *Convention Concerning The Protection of The World Cultural and Natural Heritage*, http://whc.unesco.org/en/convention text/. (30 December 2013).

[9] National Library of Indonesia, *Indonesian Temples*, http://candi.pnri.go.id/jawa barat/index.htm. (25 November 2013).

[10] Google maps, *Cangkuang Temple Location, Garut City*, http://maps.google. com/ maps. (5 September 2014).

[11] Reshetyuk, Y., *Terrestrial Laser Scanning, Error Source, Self-calibration, And Direct Geo referencing, 1st Ed.*, VDM Verlag Dr. Muller-Saarbrucken Tyskland, p. 184, 2009.

[12] Fröhlich, C. & Mettenleiter, M., *Terrestrial Laser Scanning, New Perspectives in 3D Surveying*, Proceeding International Archive of the Photogrammetry, Remote Sensing and Spatial Information Sciences

(ISPRS), Laser-Scanners for Forest and Landscape Assessment 03-06 October, 2004, M. Thies, B. Koch, H. Spiecker, H. Weinacker, (eds.), **XXXVI–8/W2**, pp. 1-7, 2004.

[13] Slob, S. & Hack, R., *3D Terrestrial Laser Scanning as New Field Measurement and Monitoring Techniqu*e, Lecture Notes in Earth Sciences, Engineering Geology for Infrastructure Planning in Europe, Springer, New York, **104**, pp. 179-189, 2004.

[14] Quintero, M., Genechten, B.V., Bruyne, M.D., Ronald, P., Hankar, M. & Barnes, S., *Theory And Practice On Terrestrial Laser Scanning*, Learning Tools for Advanced Three-dimensional Surveying in Risk Awareness Project (3DRiskMapping), 2008.

[15] Topcon, Leaflet GLS-1000–*Geodetic Laser Scanner*, Topcon Positioning System Inc., ©2008 Topcon Corporation, http://www.topcontotalcare.com/en/hardware/scanning/gls_1000/specifications/.(30 December 2013).

[16] Topcon, *Leaflet IS – Imaging Station: Long Range Scanning-Imaging and Robotic Total Station*, Topcon Positioning System Inc., ©2008 Topcon Corporation, http://www. topconpositioning.com/products/total-stations/imaging-and-scanning/ imaging-station. (30 December 2013).